Available online at www.sciencedirect.com
SCIENCE DIRECT®
Journal of Organometallic Chemistry 690 (2005) 1800–1806
Journal of Organometallic Chemistry
www.elsevier.com/locate/jorganchem

Organotin flufenamates: Synthesis, characterization and antiproliferative activity of organotin flufenamates

Dimitra Kovala-Demertzi [a,*], Vaso N. Dokorou [a], Jerry P. Jasinski [b], Adam Opolski [c], Joanna Wiecek [a], Maria Zervou [d], Mavroudis A. Demertzis [a,*]

[a] Inorganic and Analytical Chemistry, Department of Chemistry, University of Ioannina, 45110 Ioannina, Greece
[b] Department of Chemistry, Keene State College, 229 Main Street, Keene, NH 03435-2110, USA
[c] Institute of Immunology and Experimental Therapy, Polish Academy of Sciences, Weigla 12, 53-114 Wroclaw, Poland
[d] National Hellenic Research Foundation, Institute of Organic and Pharmaceutical Chemistry, Vas. Constantinou 48, 11635 Athens, Greece

Received 2 February 2005; accepted 2 February 2005
Available online 16 March 2005

Abstract

The organotin flufenamates $[Me_2(flu)SnOSn(flu)Me_2]_2$ (**1**), $[Bu_2(flu)SnOSn(flu)Bu_2]_2$ (**2**) and $[Bu_2Sn(flu)_2]$ (**3**) have been prepared and structurally characterized by means of vibrational and NMR (^1H, ^{13}C and ^{119}Sn) spectroscopy. The crystal structure of $[Me_2(flu)SnOSn(flu)Me_2]_2$ (**1**) has been determined by X-ray crystallography. Three distannoxane rings are present to the dimeric tetraorganodistannoxane of planar ladder arrangement. The structure is centro-symmetric and features a central rhombus Sn_2O_2 unit with two additional tin atoms linked at the O atoms. Six-coordinated tin centers are present in the dimer distannoxane. This structure is self-assembled via $\pi \rightarrow \pi$ and C–H $\rightarrow \pi$ stacking interactions. Flufenamic acid and flufenamates were evaluated for antiproliferative activity in vitro. Among the compounds tested $[Bu_2(flu)SnOSn(flu)Bu_2]_2$ (**2**) and $[Bu_2Sn(flu)_2]$ (**3**) exhibited high cytotoxic activity against the cancer cell line A549 (non-small cell lung carcinoma).

Keywords: Flufenamic acid; Diorganotin flufenamates; Crystal structure; Spectroscopic studies; Antitumor agents

1. Introduction

Organotin compounds are of interest in view of their considerable structural diversity. Among the compounds, the most ubiquitous are the carboxylates [1]. The reactions of precursors with carboxylic acids have been studied in considerable detail. Depending on the carboxylic acid used and the stoichiometry of the reactants, several products such as monomers, dimers, tetramers, oligomeric ladders, and hexameric drums have been isolated [1]. The increasing interest in organotin(IV) carboxylates that has arisen in the last few decades is attributed to their significantly important biological properties. Several di- and tri-species have shown potential as antineoplastic and antituberculosis agents [2].

Flufenamic acid (*N*-[3-(trifluoromethyl)-phenyl]-anthranilic acid), Hflu (Scheme 1), belongs to the class of non-steroidal anti-inflammatory drugs, NSAIDs, which are clinically used against a wide range of acute and chronic disorders. The therapeutic activity of these analgesics is believed to be due to their ability to inhibit the biosynthesis of prostaglandins by competitive interaction with the cyclooxygenase–arachidonic acid complex or by radical quenching agents that interfere with the initiation of the cyclooxygenase reaction [3]. Additionally, Hflu produces inhibition of a variety of

* Corresponding authors. Tel.: +30 651 98425; fax: +30 651 98792 (D. Kovala-Demertzi), Tel.: +30 651 98425; fax: +30 651 44831 (M.A. Demertzis).
E-mail addresses: dkovala@cc.uoi.gr (D. Kovala-Demertzi), mdemert@cc.uoi.gr (M.A. Demertzis).

0022-328X/$ - see front matter © 2005 Elsevier B.V. All rights reserved.
doi:10.1016/j.jorganchem.2005.02.004

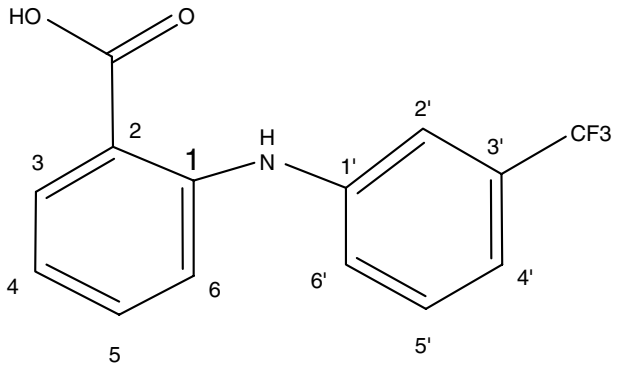

Scheme 1.

ion channel responses in a range of tissues. These actions are capable of encompassing both anion and cation channels and it appears that ion channels are the targets of the drug [4,5]. Flufenamic acid was found to inhibit the proliferation and migration of human aortic smooth muscle cells (haSMCs) in vitro [5c]. The crystal structure of Hflu [6] and of flufenamic acid with prostaglandin D (2) 11-ketoreductase (AKR1C3) has been reported [7].

Given the pharmacological importance of flufenamic acid and the potential biological activity of carboxylates, it was thought of interest to explore the chemistry of/flufenamic acid compounds. In order to widen the scope of investigations on the coordination behavior of non-steroidal anti-inflammatory drugs, NSAIDs, towards organotins, we carried out systematic studies of organotin(IV) derivatives of oxicams and fenamates [8,9], with the final goal to develop new biologically active pharmaceuticals. Here, we report the synthesis and structural studies of the novel complexes $[R_2(flu)SnOSn(flu)R_2]_2$ R = Me (**1**), Bu (**2**) and $[Bu_2Sn(flu)_2]$ (**3**). The complexes have been structurally characterized by means of vibrational and ^1H, ^{13}C and ^{119}Sn NMR spectroscopic studies. The crystal and molecular structure of **1** is described. The results of the cytotoxic activity of flufenamic and flufenamates against the cancer cell line A549 (non-small cell lung carcinoma) are also reported. These are the first reported complexes and crystal structure of a flufenamic complex.

2. Experimental

2.1. General and instrumental

The reagents (Aldrich, Merck, Sigma) were used as supplied while the solvents were purified according to standard procedures. Melting points were determined in open capillaries and are uncorrected. Infrared and far-infrared spectra were recorded on a Nicolet 55XC Fourier transform spectrophotometer using KBr pellets (4000–400 cm^{-1}) and nujol mulls dispersed between polyethylene disks (400–40 cm^{-1}). The ^1H (250.13 MHz), ^{13}C (62.90 MHz) NMR spectra were recorded on a Bruker AMX-400 and on a Bruker AC-250 spectrometer. ^{119}Sn spectra were recorded on a Bruker AC-300 spectrometer operating at 111.9 MHz. The spectra were acquired at room temperature (298 K). The chemical shifts are reported in ppm with respect to the references (external tetramethylsilane (TMS) for ^1H and ^{13}C NMR and neat tetramethyltin for ^{119}Sn). Samples were dissolved in $CDCl_3$ and spectra were obtained at room temperature with the signal of free $CDCl_3$ (at 7.24 ppm) as a reference. Elemental analyses were carried out by the microanalytical service of the University of Ioannina, Greece.

2.2. Synthesis

2.2.1. *[Me$_2$(flu) SnOSn(flu)Me$_2$]$_2$ (1)*

Dimethyltin(IV) oxide (0.198 g, 1.2 mmol) and flufenamic acid (0.281 g, 1.0 mmol) in benzene (40 ml) were refluxed for 24 h under azeotropic removal of H_2O (*Dean–Stark* trap). The resulting clear solution was concentrated in vacuo to a small volume. The oily product was chilled and triturated with diethyl ether (Et_2O) to give a yellow solid. The yellow powder was dried in vacuo over silica gel. Yield 26%; m.p. 216 °C. IR: 3312 ν(NH), 1611, 1585 ν_{as}(COO), 1395, 1462 ν_{sym}(COO); 589, 577, 547 ν(Sn–C); 648, 621 ν(Sn–O)$_2$; 300sh, 277 ν(Sn–O); 176, 153 δ(Sn–O). Crystals of **1** suitable for X-ray analysis were obtained by slow evaporation of a fresh tetrahydrofurane/acetone (1:1) solution Anal. calc. for $C_{64}H_{60}N_4O_{10}F_{12}Sn_4$ (1747.8 g mol^{-1}): C, 44.0; H, 3.5; N, 3.2. Found: C, 44.4; H, 3.6; N, 3.0%.

2.2.2. *[Bu$_2$(flu)SnOSn(flu)Bu$_2$]$_2$ (2) and [Bu$_2$Sn(flu)$_2$] (3)*

Di-*n*-butyltin(IV) oxide (0.286 g, 1.15 mmol) and flufenamic acid (0.281 g, 1.0 mmol) for **2** and (0.605 g, 2.15 mmol) for **3** in benzene (40 ml) were refluxed for 24 h under azeotropic removal of H_2O (*Dean–Stark* trap). The resulting clear solutions were concentrated in vacuo to a small volume. The oily products were chilled and triturated with trifluoroacetic acid (TFA) to give a yellow and bright yellow powder, respectively, for **2** and **3**. The powders were dried in vacuo over silica gel. $[Bu_2(flu)SnOSn(flu)Bu_2]_2$ (**2**): Yield 82%; m.p. 52–55 °C. IR: 3317 ν(NH), 1685, 1609 ν_{as}(COO), 1413, 1464 ν_{sym}(COO); 544, 520, 482 ν(Sn–C); 636, 617 ν(Sn–O)$_2$; 299, 285sh ν(Sn–O); 171, 157 δ(Sn–O). Anal. calc. for $C_{88}H_{108}N_4O_{10}F_{12}Sn_4$ (2084.4 g mol^{-1}): C, 50.7; H, 5.2; N, 2.7. Found: C, 51.0; H, 5.4; N, 2.6%. $[Bu_2Sn(flu)_2]$ (**3**): Yield 77%; m.p. 77–78 °C; IR (KBr): 3314 ν(NH), 1671 ν_{as}(COO), 1412 ν_{sym}(COO); 543, 519 ν(Sn–C); 302, 287sh ν(Sn–O); 177, 154 δ(Sn–O). Anal. calc. for $C_{36}H_{36}N_2O_4F_6Sn_1$ (793.4 g mol^{-1}): C, 54.5; H, 4.6; N, 3.5. Found: C, 54.2; H, 4.5; N, 3.3%.

2.3. X-ray crystallography

The crystallographic data for **1** are given in Table 1, together with refinement details. All measurements were performed on a *Rigaku AFC6S* diffractometer, with graphite-monochromated Mo Kα radiation. The data were collected in the ω–2θ scan technique to a maximum 2θ value of 55.0°. The structure **1** was solved by direct methods and expanded by *Fourier* techniques [10]. The non-hydrogen atoms were refined anisotropically. Hydrogen atoms were refined in their calculated positions as "riding atoms". The two sets of fluoro atoms were disorded and were refined anisotropically but in "restrained format" (C–F distance 1.40 Å and σ 0.001). All calculations were performed with the teXsan [10] crystallographic software package (Molecular Structure Corporation), except for refinement, which was performed with SHELXL-97 [11].

2.4. Antiproliferative assay in vitro

2.4.1. Compounds

Test solutions of the compounds tested (1 mg/ml) were prepared ex tempore by dissolving the substance in 100 μl of DMSO completed with 900 μl of tissue culture medium. Afterwards, the tested compounds were diluted in culture medium to reach the final concentrations of 100, 10, 1, and 0.1 μg/ml. The solvent (DMSO) in the highest concentration used in test did not reveal any cytotoxic activity.

Table 1
X-ray crystal data and structure refinement

	1
Crystallized from	THF/acetone
Crystal size (mm)	$0.30 \times 0.40 \times 0.50$
Formula	$C_{64}H_{60}N_4O_{10}F_{12}Sn_4$
M_r	1747.8
T (K)	293(2)
Wavelength (Å)	0.71073
Crystal system	Triclinic
Space group	$P\bar{1}$ (No. 2)
Cell dimensions	
a (Å)	9.2782(19)
b (Å)	13.269(3)
C (Å)	15.530(3)
α (°C)	64.99(3)°
β (Å)	83.78(3)°
γ (Å)	77.99(3)°
V (Å^3)	1694.4(6)
Z	1
D_{calc} (Mg m^{-3})	1.713
Absorption coefficient (mm^{-1})	1.548
F(000)	860
θ Range (°)	1.72–27.50
Ranges of hkl	$-12 \leqslant h \leqslant 11$, $-17 \leqslant k \leqslant 0$, $-20 \leqslant l \leqslant 18$
Reflections collected	8096
Independent reflections [R_{int}]	7760 [0.0911]
Refinement	Full-matrix least-squares on F^2
Data/restraints/parameters	7760/54/492
Goodness-of-fit (F^2)	0.959
Final R_1/w_2 indices ($I > 2\sigma_I$)	0.0400, 0.0869
Largest diff. peak/hole (e Å^{-3})	0.696 and −0.711

2.4.2. Cells

The established in vitro human cancer cell line, A549 (non-small cell lung carcinoma), was applied: The line was obtained from the American Type Culture Collection (Rockville, MD, USA) and is maintained in the Cell Culture Collection of the Institute of Immunology and Experimental Therapy, Wroclaw, Poland. Twenty-four hours before addition of the tested agents, the cells were plated in 96-well plates (Sarstedt, USA) at a density of 10^4 cells per well. The cells were cultured in the opti-MEM medium supplemented with 2 mM glutamine, streptomycin (50 μg/ml), penicillin (50 U/ml) and 5% fetal calf serum. The cell cultures were maintained at 37 °C in humid atmosphere saturated with 5% CO_2.

2.4.3. SRB assay

The details of this technique were described by Skehan et al. [12]. The cytotoxicity assay was performed after 72-h exposure of the cultured cells to varying concentrations (from 0.1 to 100 μg/ml) of the tested agents. The cells attached to the plastic were fixed by gently layering cold 50% trichloroacetic acid (TCA) on the top of the culture medium in each well. The plates were incubated at 4 °C for 1 h and then washed five times with tap water. The background optical density was measured in the wells filled with culture medium, without the cells. The cellular material fixed with TCA was stained with 0.4% sulforhodamine B dissolved in 1% acetic acid for 30 min. Unbound dye was removed by rinsing (4×) with 1% acetic acid. The protein-bound dye was extracted with 10 mM unbuffered Tris base for determination of optical density (at 540 nm) in a computer-interfaced, 96-well microtiter plate reader Multiskan RC photometer (Labsystems, Helsinki, Finland). Each compound in given concentration was tested in triplicates in each experiment, which was repeated 3–5 times.

3. Results and discussion

3.1. Crystal structure of *1*

The molecular structure of **1** is shown in Fig. 1 and selected interatomic parameters are collected in Table 2. Compound **1** is a centrosymmetric dimer distannoxane built up around the planar cyclic Sn_2O_2 unit. The two oxygen atoms of this unit are tridentate as they link three Sn centers, two endo-cyclic and one exo-cyclic. The distance between the endocyclic and exocyclic tin

atoms is 3.732(1) and the distance between the two endocyclic tin centers is 3.290(1). The additional links between the endo- and exo-cyclic Sn atoms are provided by bridging carboxylato ligands that form asymmetrical bridges (Sn(1A)–O(1B) 2.340(5) Å and Sn(1B)–O(2B) 2.204(5) Å). Each exocyclic Sn atom is also coordinated by an anisobidentate chelating carboxylato ligand (Sn(1A)–O(1A) 2.172(5) Å and Sn(1A)–O(2A) 2.783(5) Å). This distance of 2.783(5) and the Sn(1B)–O(1Aa) distance of 2.871(4) Å are considered long to indicate significant bonding interactions, however, the range of distances Sn–O of 2.61–3.02 Å has been confidently reported for intramolecular bonds [13].

The structures of dimeric distannoxane of anthranilic acid, $[Me_2(NH_2\text{-}o\text{-}H_4C_6CO_2)SnOSn(NH_2\text{-}o\text{-}H_4C_6CO_2)Me_2]_2$ [14] and of $[Bu_2(DMPA)SnOSn(DMPA)Bu_2]_2$ HDMPA is 2-[bis(2,6-dimethylphenyl)amino]benzoic acid [8d] have solid state structure closely resembling the **1**, both in the geometry of the central core $(Sn_2O_2)_2$, the coordination mode of anthranilic acid and the presence of weaker interactions (2.736(9)–2.918(6)). The anisobidentate chelated carboxylato of **1** has a difference of 0.053 Å between its C–O bonds while for the bidentate bridged carboxylato this difference is only 0.019 Å; the variations in the C–O bond distances suggest charge delocalization over the carboxylato group COO. The relevant bond lengths thus easily differentiate the different modes of bonding of the carboxylate, i.e., bridging or chelating.

The phenyl rings are planar. The dihedral angles between the planes of the phenyl rings for **1** are 44.7(4)° and 40.4(4)° for the bidentate bridging and the anisobidentae chelating ligands, respectively. The angles between the two phenyl rings are 53° and 44° in the two conformers of flufenamic [4]. The aminobenzoate portion of each carboxylato ligand is effectively planar which presumably facilitates the formation of intramolecular hydrogen bonding N(1A)–H···O(2A) and N(1B)–H···O(1B) interactions of 2.660(8) and 2.685(8) Å, respectively. The crystal structure of **1** shows ring-stacking interactions. The monomers are stacked by a strong $\pi \rightarrow \pi$ interaction and weaker C–H $\rightarrow \pi$ interactions. In this case complex **1** is self-assembled via C–H $\rightarrow \pi$ and $\pi \rightarrow \pi$ stacking interactions. C–H $\rightarrow \pi$, $\pi \rightarrow \pi$ stacking and intramolecular hydrogen interactions stabilize this structure, Table 3. The overall geometry found in **1**, allowing for differences in chemistry, is remarkably similar to compounds with the general formula $[R_2(R'CO_2)SnOSn(O_2CR')R_2]_2$ [1b,1c].

3.2. Spectroscopic studies

In the IR spectrum of Hflu, the strong band at 3320 cm^{-1} was assigned to the N–H stretching motion,

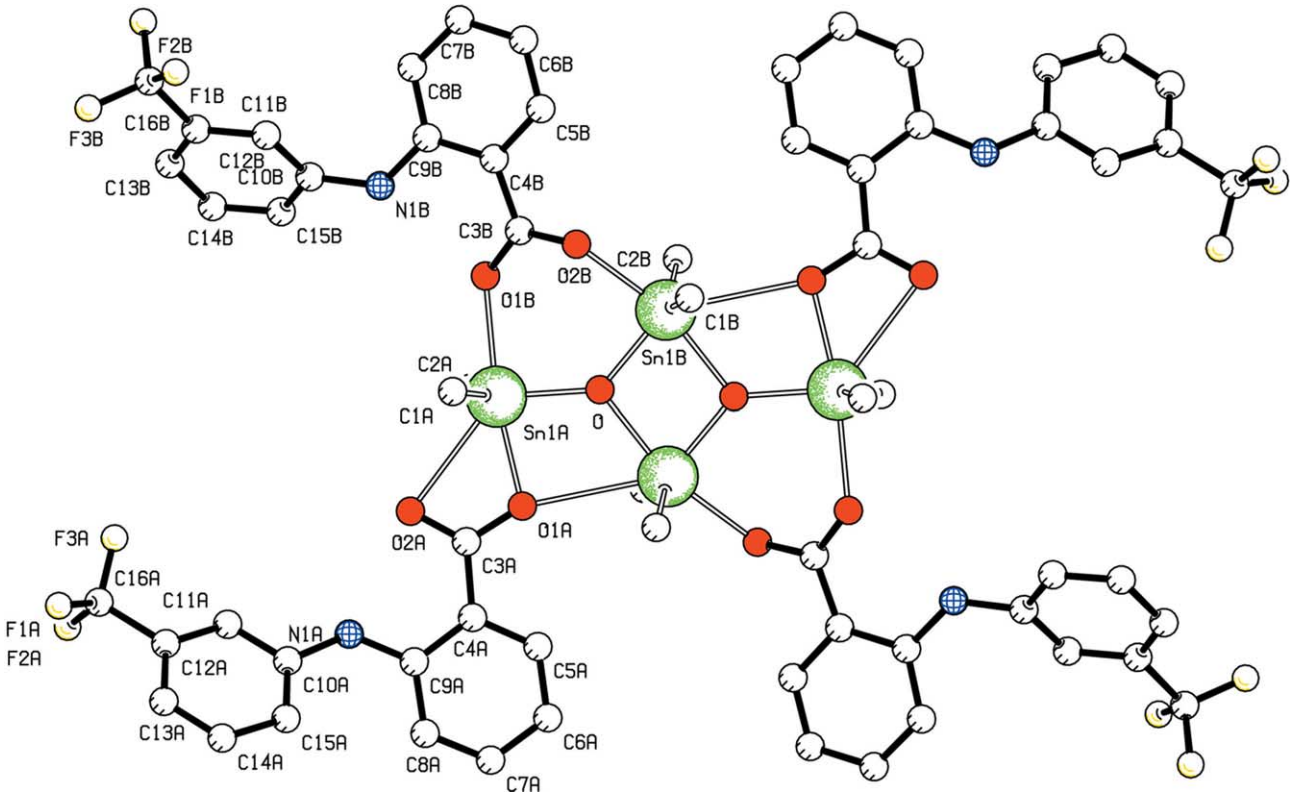

Fig. 1. Perspective view of **1** showing the atomic numbering scheme.

Table 2
Bond lengths (Å) and angles (°) for **1**

Sn(1A)–O	2.024(4)
Sn(1A)–C(2A)	2.096(8)
Sn(1A)–C(1A)	2.111(8)
Sn(1A)–O(1A)	2.172(5)
Sn(1A)–O(1B)	2.340(5)
Sn(1B)–O	2.033(4)
Sn(1B)–C(2B)	2.092(8)
Sn(1B)–C(1B)	2.101(8)
Sn(1B)–$O^{\#1}$	2.154(5)
Sn(1B)–O(2B)	2.204(5)
O–Sn(1A)–C(2A)	110.2(3)
O–Sn(1A)–C(1A)	106.0(2)
C(2A)–Sn(1A)–C(1A)	142.6(3)
O–Sn(1A)–O(1A)	80.5(2)
C(2A)–Sn(1A)–O(1A)	96.8(3)
C(1A)–Sn(1A)–O(1A)	98.4(3)
O–Sn(1A)–O(1B)	91.5(2)
C(2A)–Sn(1A)–O(1B)	83.1(3)
C(1A)–Sn(1A)–O(1B)	86.7(3)
O(1A)–Sn(1A)–O(1B)	171.5(2)
O–Sn(1B)–C(2B)	105.8(3)
O–Sn(1B)–C(1B)	112.9(2)
C(2B)–Sn(1B)–C(1B)	140.7(3)
O–Sn(1B)–$O^{\#1}$	76.44(17)
C(2B)–Sn(1B)–$O^{\#1}$	99.0(3)
C(1B)–Sn(1B)–$O^{\#1}$	96.3(2)
O–Sn(1B)–O(2B)	89.1(2)
C(2B)–Sn(1B)–O(2B)	90.7(3)
C(1B)–Sn(1B)–O(2B)	83.5(3)
$O^{\#1}$–Sn(1B)–O(2B)	164.3(2)

Symmetry transformations used to generate equivalent atoms: $^{\#1}-x+2, -y+1, -z+1$.

Table 3
C–H/π Interactions and intramolecular H-bonds and distances (···) *for* **1**

X	H	Z	H···Z	X···Z	∠(X–H···Z)
C–H/π (**1**)					
C(1A)[i]	H(1A)	Cg(6)[a]	2.967	3.680(9)	132.13
C(11A)[ii]	H(11A)	Cg(3)[a]	3.088	3.657(9)	121.09
C(13A)[iii]	H(13A)	Cg(4)[a]	3.199	3.814(12)	125.29
		Cg–Cg[b]	β[c]	CgI-Perp[d]	CgJ-Perp[d]
Cg(6)[iv] → Cg(6)		3.740(4)	11.42	3.666	3.666
H-bonds (**1**)					
N(1A)	H(1A)	O(2A)	2.07(9)	2.660(8)	141(8)
N(1B)	H(1B)	O(1B)	2.00(7)	2.685(8)	141(7)
C(5A)	H(5A)	O(1A)	2.42	2.750(10)	101
C(5B)	H(5B)	O(2B)	2.37	2.713(10)	101

Distances in Å, angles in degrees (°); X is a C-, O-, or N-atom, Z is either a centroid (Cg) or an O-atom. See Fig. 1 for atom numbering.
[a] Cg(3), Cg(4) and Cg(6) refer to the centroids C(4A)···C(9A), C(4B)···C(9B) and (10B)···C(15B).
[b] Cg–Cg is the distance between ring centroids; symmetry transformations: (i) $1+x,y,z$; (ii) $2-x, 2-y, -z$; (iii) $2-x, 1-y, -z$; (iv) $1-x, 1-y, -z$.
[c] β is the angle Cg(I) → Cg(J).
[d] CgI-Perp or CgJ-Perp is the perpendicular distance of Cg(I) on ring J.

and the broad band at ca. 2870 cm^{-1} to the ν(NH···O) and ν(OH···O) mode due to intra- and intermolecular H-bonding, as confirmed by X-ray crystallography [6]. The absence of large systematic shifts of the ν(NH) and δ(NH) bands in the spectra of the complexes compared with those of the ligand indicates that there is no interaction between the NH group and the metal ions. The ν_{asym}(COO) and ν_{sym}(COO) bands appear at ca. 1680–1580 and 1450–1300 cm^{-1}, respectively. The ν_{as}(COO) bands appear at 1681, 1609 and at 1611, 1585 $cm^{-1}$for **1** and **2**, respectively, and ν_{sym}(COO) at 1413, 1464 and at 1395, 1462 cm^{-1} for **1** and **2**, respectively. The difference $\Delta[\nu_{as}(COO) - \nu_{sym}(COO)]$ between these frequencies for **1** (276, 123 cm^{-1}) and **2** (272, 135 cm^{-1}) is close to that found for anisobidentate chelate mode (276, 272 cm^{-1}) and bridging bidentate carboxylato groups (123, 135 cm^{-1}). This is totally consistent with the X-ray structure of **1**. The ν_{asym}(COO) and ν_{sym}(COO) bands appear at 1671 and 1412 cm^{-1} for **3**. The difference $\Delta[\nu_{asym}(COO) - \nu_{sym}(COO)]$ between these frequencies is 259 cm^{-1}, which is close to that found for the anisobidentate chelate carboxylato group. Two bands at 650–620 cm^{-1} for **1** and **2** are assigned to symmetric and asymmetric $(SnO)_2$ vibrations, indicating nonlinear O–Sn–O moieties. The bands at 300–280 cm^{-1} are assigned to the Sn–O(COO) stretching modes. The absorption bands at 540–500 cm^{-1} are attributed to ν(Sn–C) stretching modes [8,9,15].

The ^{1}H and ^{13}C NMR data for flufenamic acid and the complexes are summarized in Table 4. These results, together with the published data on flufenamic acid [16], allowed complete assignment of all signals in the spectra of both the flufenamic acid and complexes. The downfield chemical shift for HN in flufenamic acid indicates that this proton is involved in hydrogen bonding. The crystal structure of flufenamic acid suggests the presence of hydrogen-bonded dimers linked by two intermolecular O–H–O hydrogen bonds and an intramolecular hydrogen bond between the HN group and the carbonyl group of the carboxyl acid [6]. The existence of the HN resonance in the ^{1}H NMR spectra indicates that the nitrogen atoms remain protonated in **1**–**3**. In the ^{1}H NMR spectrum of **1**, three singlets appear in the region of the tin-bound methyl groups, but integration shows that in the case of the signal emerging at 1.25 ppm, two methyl groups are present indicating accidental equivalence. Deshielding of protons H(3) and H(4) is observed in complexes, which should be related to the electrophilicity of the tin. A σ-charge donation from the COO-donor to the tin center removes electron density from the ligand and produces this deshielding which will attenuate at positions remote from the metal. The remaining resonances due to the aromatic carbon atoms do not shift significantly on binding to Sn. The ^{13}C NMR spectra of **2** and **3** reveal resonance assignable to the $\underline{C}O_2$ nucleus and coordination is confirmed by the fact that this resonance exhibits a downfield shift. Involvement of the

Table 4
^{1}H, ^{13}C and ^{119}Sn NMR data[a]

	COOH	NH	H3	H4	H6	H5, H2′, H4′–H6′	^{119}Sn
Hflu[c]		9.39s	8.09dd	6.74t	7.29d	7.32–7.51m	
1[b]	Me_2Sn 1.05s/1.54s 1.26s/1.26s	9.87br	7.93br	6.76br	7.29d	7.32–07.50m	
2	Bu_2Sn	9.26br	8.11d	6.85t	7.26d	7.35–7.51m	
	Hδ: 0.91, Hγ: 1.26						−121.5
	Hβ: 1.80, Hα: 1.40						−173.9
3	Bu_2Sn	8.47br	8.13d	6.86t	7.26t	7.33–7.50m	
	Hδ: 0.91, Hγ: 1.43						−112.9
	Hβ: 1.85, Hα: 1.75						

	COOH	C1	C2	C3	C4	C5	C6	C1′	C2′	C3′	C4′	C5′	C6′	CF_3
Hflu	174.0	147.6	111.3	132.8	118.4	135.4	114.2	141.1	118.8	131.9	120.1	129.9	125.2	121.7
2	177.6	147.4	112.7	133.8	118.6	135.6	114.1	141.3	118.5	131.8	120.1	129.8	125.1	121.8
	Bu_2Sn Cδ: 13.5, Cγ: 22.7, Cβ: 29.7, Cα: 31.9													
3[c]	Bu_2Sn Cδ: 13.4, Cγ: 26.3, Cβ: 26.5, Cα: 29.8 COOO: 175.5	147.7	111.1	133.3	118.7	135.7	114.1	141.2	118.4	131.8	120.1	129. 9	125.2	122.5

[a] Spectra recorded in $CDCl_3$.
[b] In $CDCl_3$ and d_6-DMSO insufficient solubility to record a measurable ^{13}C and ^{119}Sn NMR spectrum.
[c] Carboxyl proton exchanged in $CDCl_3$.

carboxyl group in bonding to Sn is confirmed by the resonance ascribed to C(2), which exhibit the greatest shift upon coordination. The remaining resonances due to the aromatic carbon atoms do not shift significantly on binding to Sn. The ^{119}Sn chemical shifts of tin complexes appear to depend not only on coordination number, but also on the type of donor atoms bonded to the metal ion. As reported in the literature, [17a] chemical shifts in the range δ −210 to −400 ppm, −90 to −190 ppm and 200 to −60 ppm have been associated with six-, five- and four-coordinate tin centers, respectively. The ^{119}Sn NMR spectrum of **2** exhibits two distinct resonances at −121.5 and −173.9 confirming *endo*- and *exo*-cyclic tin atoms [1d]. The value of δ −112.9 ppm for complex **3** is within the range expected for five-coordinate complexes. The chemical shift for complex **3** in $CDCl_3$ indicates that the six-coordinate Sn atom in the solid state structure (as revealed by IR spectroscopy) is lost upon dissolution giving rise to a five-coordinate tin atom in solution. This change could be explained by the rupture of the weak Sn–O bond in solution [17b,8d].

3.3. Antiproliferative activity in vitro of organotin complexes

The results of cytotoxic activity in vitro are expressed as ID_{50} – the dose of compound (in μg/ml) that inhibits a proliferation rate of the tumor cells by 50% as compared to control untreated cells. Flufenamic acid, Hflu, and flufenamates **2** and **3** exhibited cytotoxic activity against the human lung cancer cell line A549 (see Table 5). The ID_{50} value for **2** and **3** are lower to the international activity criterion for synthetic agents (4 μg/ml) [18]. Thus, compounds **2** and **3** are considered as agents with potential antitumor activity, and can therefore be candidates for further stages of screening in vitro and/or in vivo.

Table 5
The antiproliferative activity in vitro of Hflu, and flufenamates **2** and **3** (expressed as ID_{50}) against A-549 lung human cancer cell line[a]

Compounds	$ID_{50} \pm SD$ (μg/ml)
Hflu	30.0 ± 1.0
$[Bu_2(flu)SnOSn(flu)Bu_2]_2$	0.24 ± 0.1
$[Bu_2Sn(flu)_2]$	0.35 ± 0.1
Carboplatin	108.0

[a] Unsufficient solubility of **1** in DMSO to perform the antiproliferative activity.

3.4. Conclusions

Three novel flufenamates $[Me_2(flu)SnOSn(flu)Me_2]_2$ (**1**), $[Bu_2(flu)SnOSn(flu)Bu_2]_2$ (**2**) and $[Bu_2Sn(flu)_2]$ (**3**) have been prepared and structurally characterized by means of vibrational, ^{1}H NMR, ^{13}C NMR and ^{119}Sn NMR spectroscopy. Based on spectroscopic data, dimeric tetraorganostannoxanes are proposed for **1** and **2**, and monomeric hexa-coordinate structure for **3**, respectively. The crystal structure of **1** was determined by X-ray crystallography. Flufenamic acid and flufenamates **2** and **3** were evaluated for antiproliferative activity in vitro. Among the compounds tested **2** and **3** exhibited high cytotoxic activity against the cancer cell line A549 (non-small cell lung carcinoma) and compounds **2** and **3** are considered as agents with potential

antitumor activity, and can therefore be candidates for further stages of screening in vitro and/or in vivo.

4. Supplementary material

Crystallographic data for the structural analyses have been deposited at *Cambridge Crystallographic Data Centre*, as deposition number CCDC-247773. Copies of these data may be obtained, free of charge, from CCDC, 12 Union Road, Cambridge CB2 1EZ, UK, via fax: (+44 1223 336 033), e-mail (deposit@ccdc.cam.ac.uk), or internet (www.ccdc.cam.ac.uk).

Acknowledgments

This research was funded by the program "Heraklitos" of the Operational Program for Education and Initial Vocational Training of the Hellenic Ministry of Education under the 3rd Community Support Framework and the European Social Fund.

References

[1] (a) R.R. Holmes, Acc. Chem. Res. 22 (1989) 190;
(b) E.R.T. Tiekink, Appl. Organomet. Chem. 5 (1991) 1;
(c) E.R.T. Tiekink, Trends Organomet. Chem. 1 (1994) 71;
(d) V. Chandrasekhar, S. Nagendran, V. Baskar, Coord. Chem. Rev. 235 (2002) 1;
(e) G. Prabusankar, R. Murugavel, Organometallics 23 (2004) 5644, and references therein.

[2] (a) M. Gielen, Appl. Organomet. Chem. 16 (2002) 481;
(b) M. Gielen, Coord. Chem. Rev. 15 (1996) 41;
(c) A.J. Crowe, in: M. Gielen (Ed.), Metal-based Antitumour Drugs, vol. 1, Freund, London, 1989;
(d) D. Kovala-Demertzi, V. Dokorou, Z. Ciunik, N. Kourkoumelis, M.A. Demertzis, Appl. Organomet. Chem. 16 (2002) 360;
(e) V. Dokorou, D. Kovala-Demertzi, J.P. Jasinski, A. Galani, M.A. Demertzis, Helv. Chim. Acta 87 (2004) 1940.

[3] (a) M. Ouellet, M.D. Percival, Biochem. J. 306 (1995) 247;
(b) Th. Nogrady, Medicinal chemistry, second ed., Oxford University Press, Oxford, 1998.

[4] (a) H. Kankaanranta, M. Luomala, O. Kosonen, E. Moilanen, Br. J. Pharmacol. 119 (1996) 487;
(b) H. Kankaanranta, E. Moilanen, Mol. Pharmacol. 47 (1995) 1006.

[5] (a) S.L. Grage, D.R. Gauger, C. Selle, W. Pohle, W. Richter, A.S. Ulrich, Phys. Chem. Chem. Phys. 2 (2000) 4574, and references therein;
(b) N. Parij, A.-M. Nagy, P. Fondy, J. Neve, Eur. J. Pharmacol. 352 (1998) 299;
(c) W. Schober, J. Wiskirchen, R. Kehlbach, R. Gebert, E. Rodegerdts, A. Betsch, U. Johst, C.D. Claussen, S.H. Duda, J. Vasc. Intervent. Radiol. 13 (1) (2002) 89.

[6] H.M. Krishna Murthy, T.N. Bhat, M. Vijayan, Acta Crystallogr. Sect. B 38 (1982) 315.

[7] A.L. Lovering, J.P. Ride, C.M. Bunce, J.C. Desmond, S.M. Cummings, S.A. White, Cancer Res. 64 (2004) 1802.

[8] (a) M.A. Demertzis, S.K. Hadjikakou, D. Kovala-Demertzi, A. Koutsodimou, M. Kubicki, Helvet. Chim. Acta 83 (2000) 2787;
(b) A. Galani, M.A. Demertzis, M. Kubicki, D. Kovala-Demertzi, Eur. J. Inorg. Chem. 9 (2003) 1761;
(c) S.K. Hadjikakou, M.A. Demertzis, J.R. Miller, D. Kovala-Demertzi, J. Chem. Soc., Dalton Trans. (1999) 663;
(d) V. Dokorou, M.A. Demertzis, J.P. Jasinski, D. Kovala-Demertzi, J. Organomet. Chem. 689 (2004) 317;
(e) D. Kovala-Demertzi, J. Inorg. Biochem. 79 (1–4) (2000) 153.

[9] (a) V. Dokorou, Z. Ciunik, U. Russo, D. Kovala-Demertzi, J. Organomet. Chem. 630 (2001) 205;
(b) D. Kovala-Demertzi, N. Kourkoumelis, A. Koutsodimou, A. Moukarika, E. Horn, E.R.T. Tiekink, J. Organomet. Chem. 620 (2001) 194;
(c) A. Galani, D. Kovala-Demertzi, N. Kourkoumelis, A. Koutsodimou, V. Dokorou, Z. Ciunik, U. Russo, M.A. Demertzis, Polyhedron 23 (2004) 2021.

[10] (a) teXsan for Windows version 1.06, Crystal Structure Analysis Package, Molecular Structure Corporation, 1997–1999;
(b) L.J. Farrugia, J. Appl. Cryst. 32 (1999) 837;
(c) A.L. Spek, PLATON. A program for the automated generation of a variety of geometrical entities, University of Utrecht, The Netherlands, 2002.

[11] G.M. Sheldrick, SHELXL97, Program for Crystal-structure Refinement, University of Göttingen, 1997.

[12] (a) P. Skehan, R. Storeng, D. Scudiero, A. Monks, J. Mcmahon, D. Vistica, J.T. Warren, H. Bokesch, S. Kenney, M.R. Boyol, J. Natl. Cancer. Inst. 82 (1990) 1107;
(b) A. Opolski, J. Kuduk-Jaworska, J. Wietrzyk, E. Wojdat, K. Waszkiewicz, A. Romaniewska, C. Radzikowski, Anti-Cancer Drugs 11 (2000) 363.

[13] (a) K.C. Molloy, T.G. Purcell, K. Quill, I.W. Nowell, J. Organomet. Chem. (1984) 267;
(b) A.R. Forrester, S.J. Garden, R.A. Howie, J.L. Wardell, J. Chem. Soc., Dalton Trans. (1992) 2615.

[14] V. Chandrasekhar, R.O. Day, J.M. Holmes, R.R. Holmes, Inorg. Chem. 27 (1988) 958.

[15] K. Nakamoto, Infrared and Raman Spectra of Inorganic and Coordination Compounds, fourth ed., Wiley, New York, 1980.

[16] S.L.A. Munro, D.J. Craik, Magn. Reson. Chem. 32 (1994) 335.

[17] (a) J. Holeček, M. Nádvorník, K. Handlzř, A. Lyčka, J. Organomet. Chem. 315 (1986) 299;
(b) C. Ma, J. Zhang, F. Li, R. Zhang, Eur. J. Inorg. Chem. (2004) 2775.

[18] R.I. Geran, N.H. Greenberg, M.M. Macdonald, A.M. Schumacher, B.J. Abbott, Cancer Chemother. Rep. 3 (1972) 59.